TPR-95-16

Spectral functions for composite fields and viscosity in hot scalar field theory

Enke Wang* and Ulrich Heinz

Institut für Theoretische Physik, Universität Regensburg,

D-93040 Regensburg, Germany

Xiaofei Zhang

Institute of Particle Physics, Hua-Zhong Normal University,

Wuhan 430070, China

(February 7, 2008)

Abstract

We derive a spectral representation for the two-point Green function for arbitrary composite field operators in Thermo Field Dynamics (TFD). A simple way for calculating the spectral density within TFD is pointed out and compared with known results from the imaginary time formalism. The method is applied to hot ϕ^4 theory. We give a compact derivation of the one-loop contribution to the shear viscosity and show that it is dominated by low-momentum plasmons.

PACS numbers: 11.10.-z, 51.10.+y, 52.25.Fi, 52.60.+h

I. INTRODUCTION

In the context of heavy-ion collisions at ultrarelativistic energies, transport properties of strongly interacting hot matter, in particular of the quark-gluon plasma (QGP), have become an issue of intense theoretical interest. The calculation of QGP transport coefficients from linear response functions through the Kubo-formalism [1,2] has so far been hampered by infrared problems associated with the non-linear selfinteractions among massless fields in hot QCD. A systematic and economic field theoretical approach, including resummation techniques for infrared divergences [3], to the calculation of linear response functions is clearly asked for.

As an example for the type of objects one is interested in let us take the Kubo-formula for the shear viscosity [1,4,5]

$$\eta = -\frac{1}{5}\int d^3x' \int_{-\infty}^{0} dt \int_{-\infty}^{t} dt' \, \langle \pi^{\mu\nu}(0), \pi_{\mu\nu}(\mathbf{x}', t') \rangle^{\rm ret} = \frac{\pi}{5} \lim_{\omega, \mathbf{p} \to 0} \frac{\partial \rho_{\pi\pi}(\omega, \mathbf{p})}{\partial \omega} \,. \tag{1.1}$$

Here $\pi_{\mu\nu}$ is the traceless viscous-pressure tensor which is imbedded in the energy-momentum tensor and in the comoving frame has only spatial components, π_{ij}. For a scalar field $\pi_{ij} = (\delta_{ik}\delta_{jl} - \frac{1}{3}\delta_{ij}\delta_{kl})\partial_k\phi\,\partial_l\phi$. $\rho_{\pi\pi}$ is the spectral momentum space density for the retarded thermal Green function of the composite field π, as defined below. The efficient computation of this quantity will be the subject of this paper.

The analytical structure of the retarded Green function $\langle \pi^{\mu\nu}(0), \pi_{\mu\nu}(\mathbf{x}', t') \rangle^{\rm ret}$ is similar to that of $\langle \phi^2(0), \phi^2(\mathbf{x}', t') \rangle^{\rm ret}$ [5]. The spectral density for the latter 2-point function was recently calculated at 1-loop order in the imaginary time formalism (ITF) by Jeon [5]. Here we repeat the calculation in the real-time formalism using the language of Thermo Field Dynamics (TFD) [6]. Using the analyticity properties of the 2-point functions in ITF and TFD, we give a very compact derivation of the 1-loop contribution to the spectral density of the composite field 2-point function, $\rho_{\pi\pi}$, in terms of the spectral density of the elementary field 2-point function, $\rho_{\phi\phi}$. The latter was recently calculated at 2-loop order including infrared resummation [5,7,8]. Our approach follows closely the methods developed in [9–11]

for correlation functions between elementary fields. It goes beyond the results reported in [5] in that we include the full momentum dependence of the 2-loop scalar self energy.

II. SPECTRAL REPRESENTATION OF COMPOSITE FIELD PROPAGATORS IN TFD

For two arbitrary operators $\hat{A}$, $\hat{B}$ the retarded thermal Green function is defined by

$$D^{\rm ret}_{AB}(\mathbf{r}_1-\mathbf{r}_2,t_1-t_2) = -i\theta(t_1-t_2)\,{\rm Tr}\Big(e^{\beta(\Omega-\hat{H})}[\hat{A}(\mathbf{r}_1,t_1),\hat{B}(\mathbf{r}_2,t_2)]_{\pm}\Big)\,, \tag{2.1}$$

where $\hat{H}$ is the hamiltonian, Ω is the thermodynamic potential, and the plus (minus) sign applies for fermionic (bosonic) operators $\hat{A}$, $\hat{B}$. It can be expressed as an integral over the spectral density $\rho_{AB}(\omega,\mathbf{p})$ in momentum space:

$$D^{\rm ret}_{AB}(p_0,\mathbf{p}) = \lim_{\eta\to 0^+}\int_{-\infty}^{+\infty} d\omega\,\frac{\rho_{AB}(\omega,\mathbf{p})}{p_0-\omega+i\eta}\,. \tag{2.2}$$

In the Heisenberg picture the spectral density has the Lehmann representation [12]

$$\begin{aligned}\rho_{AB}(\omega,\mathbf{p}) = (2\pi)^3\sum_{n,m} e^{\beta(\Omega-E_n)}\\ \langle n|A(0)|m\rangle\langle m|B(0)|n\rangle\,(1-\sigma e^{-\beta\omega})\,\delta(\omega-E_{mn})\,\delta^{(3)}(\mathbf{p}-\mathbf{p}_{mn})\,,\end{aligned} \tag{2.3}$$

where $\sigma=+1$ (-1) for bosonic (fermionic) operators $\hat{A}$, $\hat{B}$, respectively. The sum is over a complete set of simultaneous eigenvectors of $\hat{H}$ and $\hat{\mathbf{p}}$, with eigenvalues E_n and $\mathbf{p}_n$, and $E_{mn}=E_m-E_n$, $\mathbf{p}_{mn}=\mathbf{p}_m-\mathbf{p}_n$.

The imaginary time Green function is obtained from Eq. (2.1) by setting $it=\tau$. In momentum space it has a similar spectral representation,

$$G_{AB}(\omega_n,\mathbf{p}) = \int_{-\infty}^{+\infty} d\omega\,\frac{\rho_{AB}(\omega,\mathbf{p})}{i\omega_n-\omega}\,, \tag{2.4}$$

in terms of the same spectral function ρ_{AB}. The periodicity of the ITF Green functions in imaginary time results in the discrete Matsubara frequencies $\omega_n=2n\pi T$ and $(2n+1)\pi T$ for bosonic and fermionic operators $\hat{A}$ and $\hat{B}$, respectively. The retarded Green function (2.2) and the ITF Green function (2.4) are related by analytical continuation $i\omega_n\to p_0+i\eta$:

$$D^{\rm ret}_{AB}(p_0,\mathbf{p}) = G_{AB}(\omega_n,\mathbf{p})\Big|_{i\omega_n\to p_0+i\eta}\,. \tag{2.5}$$

The propagators in TFD have a more complicated structure: any physical field operator $\hat{A}$ is associated with a thermal ghost field operator $\tilde{A}$, with which it is combined into a doublet:

$$\begin{pmatrix} A^1 \\ A^2 \end{pmatrix} = \begin{pmatrix} \hat{A} \\ \tilde{A}^\dagger \end{pmatrix}. \tag{2.6}$$

The TFD Green function is thus a 2×2 matrix

$$\Delta^{ab}_{AB}(\mathbf{r}_1-\mathbf{r}_2,t_1-t_2) = -i\,\langle 0,\beta|T_t[\hat{A}^a(\mathbf{r}_1,t_1),\hat{B}^b(\mathbf{r}_2,t_2)]_\pm|0,\beta\rangle\,, \qquad a,b=1,2\,. \tag{2.7}$$

In momentum space it has the following spectral representation

$$\Delta^{ab}_{AB}(p_0,\mathbf{p}) = \int_{-\infty}^{+\infty} d\omega\,\left[\frac{\gamma^{ab}_{AB}(\omega,\mathbf{p})}{p_0-\omega+i\eta} - \sigma\frac{\gamma^{ba}_{BA}(\omega,-\mathbf{p})}{p_0+\omega-i\eta}\right], \tag{2.8}$$

where T_t is time ordering and the spectral function has the generalized Lehmann representation

$$\gamma^{ab}_{AB}(\omega,\mathbf{p}) = (2\pi)^3\sum_{n,m}\langle 0,\beta|A^a(0)|n,\tilde{m}\rangle\langle\tilde{m},n|B^b(0)|0,\beta\rangle\,\delta(\omega-E_{nm})\,\delta^{(3)}(\mathbf{p}-\mathbf{p}_{nm})\,, \tag{2.9}$$

$$\gamma^{ba}_{BA}(\omega,-\mathbf{p}) = (2\pi)^3\sum_{n,m}\langle 0,\beta|B^b(0)|n,\tilde{m}\rangle\langle\tilde{m},n|A^a(0)|0,\beta\rangle\,\delta(\omega-E_{nm})\,\delta^{(3)}(\mathbf{p}+\mathbf{p}_{nm})\,. \tag{2.10}$$

Here the thermal vacuum state $|0,\beta\rangle$ is defined as [6]

$$|0,\beta\rangle = \sum_k e^{\beta(\Omega-E_k)/2}|k,\tilde{k}\rangle\,, \tag{2.11}$$

where $|k,\tilde{k}\rangle = |k\rangle\otimes|\tilde{k}\rangle$, and $|\tilde{k}\rangle$ is eigenstate of $\tilde{H}$ with the same eigenvalue E_k.

Using Eq. (2.11) and the 'tilde substitution law' [6]

$$\langle 0,\beta|\tilde{A}^\dagger(0)|n,\tilde{m}\rangle = (-1)^{F_A(F_A-1)/2}\exp[-\beta E_{nm}/2]\langle 0,\beta|\hat{A}(0)|n,\tilde{m}\rangle\,, \tag{2.12}$$

$$\langle\tilde{m},n|\tilde{A}^\dagger(0)|0,\beta\rangle = (-1)^{F_A(F_A+1)/2}\exp[-\beta E_{nm}/2]\langle\tilde{m},n|\hat{A}(0)|0,\beta\rangle\,, \tag{2.13}$$

where F_A is the fermion number associated with the operator $\hat{A}$, and noticing that the physical field $\hat{A}$ only acts on the physical states $|n\rangle$ while the ghost field $\tilde{A}$ acts only on the tilde states $|\tilde{n}\rangle$,

$$\langle \tilde{k}, l|\hat{A}|n, \tilde{m}\rangle = \delta_{km}\,\langle l|\hat{A}|n\rangle\,, \tag{2.14}$$

$$\langle \tilde{k}, l|\tilde{A}|n, \tilde{m}\rangle = \delta_{ln}\,\langle \tilde{k}|\tilde{A}|\tilde{m}\rangle\,, \tag{2.15}$$

we can transform γ^{ab}_{AB} in Eqs. (2.9) and (2.10) into similar form as Eq. (2.3). Some further algebra involving Eqs. (2.2) and (2.8) then yields for the TFD propagator matrix the result

$$\Delta_{AB}(p_0,\mathbf{p}) = \tag{2.16}$$
$$\begin{pmatrix} D^{\rm ret}_{AB}(p_0,\mathbf{p}) - \dfrac{2\pi i\,\sigma}{\exp(\beta p_0)-\sigma}\rho_{AB}(p_0,\mathbf{p})\,, & -2\pi i\,\sigma\dfrac{s_{AB}\exp(\beta p_0/2)}{\exp(\beta p_0)-\sigma}\rho_{AB}(p_0,\mathbf{p}) \\ -2\pi i\,\sigma\dfrac{s_{AB}\exp(\beta p_0/2)}{\exp(\beta p_0)-\sigma}\rho_{AB}(p_0,\mathbf{p})\,, & -\sigma\left(D^{\rm ret}_{AB}(p_0,\mathbf{p})\right)^* - \dfrac{2\pi i}{\exp(\beta p_0)-\sigma}\rho_{AB}(p_0,\mathbf{p}) \end{pmatrix},$$

where $s_{AB} = (-1)^{F_A(F_A+1)/2}$, using $F_A = -F_B$ since otherwise Δ_{AB} vanishes [6].

With (2.2) this provides explicit expressions for each component of the 2-point Green function in terms of the spectral density ρ_{AB}. The relationship of ρ_{AB} to the (12)- and (21)-components of Δ_{AB} is particularly straightforward:

$$\rho_{AB}(p_0,\mathbf{p}) = s_{AB}\,\frac{i\sigma}{2\pi}\,\frac{e^{\beta p_0}-\sigma}{e^{\beta p_0/2}}\,\Delta^{12}_{AB}(p_0,\mathbf{p})\,. \tag{2.17}$$

Since the (12)-component of the 2-point Green function can be calculated directly using TFD Feynman rules, this relation provides a convenient way of obtaining the spectral density for the composite fields $\hat{A}$, $\hat{B}$.

The above expressions apply in particular to the single-particle operators $\hat{A} = \phi$ and $\hat{B} = \phi^\dagger$ ($F_A = -F_B = 0$, $\sigma = 1$). As shown in [5], $\rho_{\phi\phi^\dagger}(\omega,\mathbf{p})$ is real, depends only on $|\mathbf{p}|$ due to spatial isotropy, and is for any CPT-invariant equilibrium state an odd function of the frequency,

$$\rho_{\phi\phi^\dagger}(\omega,\mathbf{p}) = \epsilon(\omega)\rho_{\phi\phi^\dagger}(|\omega|,|\mathbf{p}|)\,, \tag{2.18}$$

where $\epsilon(\omega) = \mathrm{sgn}(\omega)$. Using Eq. (2.5) and the following relation [13] for the analytically continued ITF propagator

$$G_{\phi\phi^\dagger}(p_0+i\eta,\mathbf{p}) = G_{\phi\phi^\dagger}(p_0+i\epsilon(p_0)\eta,\mathbf{p}) + 2\pi i\theta(-p_0)\rho_{\phi\phi^\dagger}(|p_0|,\mathbf{p})\,, \tag{2.19}$$

we can write the full TFD propagator for the scalar field as

$$\Delta \equiv \Delta_{\phi\phi^\dagger}(p_0,\mathbf{p}) = \tag{2.20}$$
$$\begin{pmatrix} G_{\phi\phi^\dagger}(p_0+i\epsilon(p_0)\eta,\mathbf{p}) - \dfrac{2\pi i\,\rho_{\phi\phi^\dagger}(|p_0|,\mathbf{p})}{\exp(\beta|p_0|)-1}\,, & -2\pi i\,\dfrac{\exp(\beta|p_0|/2)}{\exp(\beta|p_0|)-1}\,\rho_{\phi\phi^\dagger}(|p_0|,\mathbf{p}) \\ -2\pi i\,\dfrac{\exp(\beta|p_0|/2)}{\exp(\beta|p_0|)-1}\,\rho_{\phi\phi^\dagger}(|p_0|,\mathbf{p})\,, & -G^*_{\phi\phi^\dagger}(p_0+i\epsilon(p_0)\eta,\mathbf{p}) - \dfrac{2\pi i\,\rho_{\phi\phi^\dagger}(|p_0|,\mathbf{p})}{\exp(\beta|p_0|)-1} \end{pmatrix},$$

with the following representations in terms of the ITF self energy Σ:

$$G_{\phi\phi^\dagger}(p_0+i\epsilon(p_0)\eta,\mathbf{p}) = \frac{1}{p^2-m^2+\mathrm{Re}\,\Sigma(|p_0|,\mathbf{p})+i\,\mathrm{Im}\,\Sigma(|p_0|,\mathbf{p})}\,, \tag{2.21}$$

$$\begin{aligned}\rho_{\phi\phi^\dagger}(|p_0|,\mathbf{p}) &= -\frac{1}{2\pi i}\left[G_{\phi\phi^\dagger}(|p_0|+i\eta,\mathbf{p}) - G_{\phi\phi^\dagger}(|p_0|-i\eta,\mathbf{p})\right] \\ &= \frac{1}{\pi}\,\frac{\mathrm{Im}\,\Sigma(|p_0|,\mathbf{p})}{\left[p^2-m^2+\mathrm{Re}\,\Sigma(|p_0|,\mathbf{p})\right]^2+\left[\mathrm{Im}\,\Sigma(|p_0|,\mathbf{p})\right]^2}\,.\end{aligned} \tag{2.22}$$

For a free scalar field both real and imaginary parts of Σ vanish, and the spectral density $\rho_{\phi\phi^\dagger}$ degenerates to a δ-function:

$$\frac{1}{\pi}\lim_{\eta\to 0}\frac{\eta}{p^2-m^2+\eta^2} = \delta(p^2-m^2)\,. \tag{2.23}$$

Eq.(2.20) in this case reduces to the free TFD propagator

$$\Delta_0 = \begin{pmatrix} \dfrac{1}{p^2-m^2+i\eta} - \dfrac{2\pi i\,\delta(p^2-m^2)}{\exp(\beta|p_0|)-1}, & -\dfrac{2\pi i\,\delta(p^2-m^2)\,\exp(\beta|p_0|/2)}{\exp(\beta|p_0|)-1} \\ -\dfrac{2\pi i\,\delta(p^2-m^2)\,\exp(\beta|p_0|/2)}{\exp(\beta|p_0|)-1}, & -\dfrac{1}{p^2-m^2-i\eta} - \dfrac{2\pi i\,\delta(p^2-m^2)}{\exp(\beta|p_0|)-1} \end{pmatrix}. \tag{2.24}$$

The full TFD propagator matrix Δ satisfies the Dyson equation [14]

$$(\Delta^{-1})^{ab} = (p^2-m^2)\tau^{ab} + \Sigma^{ab}(p_0,\mathbf{p})\,, \tag{2.25}$$

where $\tau = \mathrm{diag}(1,-1)$. This defines a 2×2 TFD self energy matrix Σ^{ab}. Comparing this with the inverse of the matrix (2.20), it is easy to obtain the following relations:

$$\mathrm{Im}\,\Sigma = \frac{e^{\beta p_0}-1}{e^{\beta p_0}+1}\,\mathrm{Im}\,\Sigma^{11} = -\frac{e^{\beta p_0}-1}{2e^{\beta p_0/2}}\,\mathrm{Im}\,\Sigma^{12}, \tag{2.26}$$

$$\mathrm{Im}\,\Sigma^{21} = \mathrm{Im}\,\Sigma^{12}, \quad \mathrm{Im}\,\Sigma^{22} = \mathrm{Im}\Sigma^{11}, \tag{2.27}$$

$$\mathrm{Re}\,\Sigma = \mathrm{Re}\,\Sigma^{11} = -\mathrm{Re}\,\Sigma^{22}\,, \quad \mathrm{Re}\,\Sigma^{12} = \mathrm{Re}\,\Sigma^{21} = 0\,. \tag{2.28}$$

They were previously obtained in [9,15] by different methods. The authors of Ref. [15] pointed out that the calculation of $\mathrm{Im}\,\Sigma$ from $\mathrm{Im}\,\Sigma^{12}$, using TFD Feynman rules for the evaluation of the latter, is particularly convenient and showed explicitly that the result is identical to the evaluation in ITF.

It is straightforward to generalize the expressions (2.20) and (2.24) as well as the self energy relationships (2.26 - 2.28) to the case of fermionic single particle operators.

III. SHEAR VISCOSITY IN HOT ϕ^4 THEORY

We will now use these results to give a five line derivation of the spectral function for the composite field ϕ^2 within hot $\lambda\phi^4$ theory. We concentrate on the same quantity as studied in Ref. [5], namely

$$\eta_{\phi^2\phi^2} \equiv \lim_{\mathbf{p},p_0\to 0}\left[\frac{\rho_{\phi^2\phi^2}(p_0,\mathbf{p})}{p_0}\right], \tag{3.1}$$

whose relation to the shear viscosity (1.1) was mentioned above. From Eq. (2.17) we obtain

$$\rho_{\phi^2\phi^2}(p_0,\mathbf{p}) = \frac{i}{2\pi}\frac{e^{\beta p_0}-1}{e^{\beta p_0/2}}\Delta^{12}_{\phi^2\phi^2}(p_0,\mathbf{p})\,. \tag{3.2}$$

The lowest order contribution to $\Delta^{12}_{\phi^2\phi^2}(p_0,\mathbf{p})$ is shown diagrammatically in Fig. 1. This is a skeleton diagram, i.e. the full single-particle propagators (2.20) must be used for the internal lines [1,5]. For the one-loop diagram in Fig. 1 only its (12)-component is needed. We find

$$\begin{aligned} i\,\Delta^{12}_{\phi^2\phi^2}(p_0,\mathbf{p}) &= 2\int\frac{d^4k}{(2\pi)^2}\left[\frac{\exp(\frac{\beta k_0}{2})\,\rho_{\phi\phi}(k_0,\mathbf{k})}{\exp(\beta k_0)-1}\right]\left[\frac{\exp(\frac{\beta(p_0-k_0)}{2})\,\rho_{\phi\phi}(p_0-k_0,\mathbf{p}-\mathbf{k})}{\exp(\beta(p_0-k_0))-1}\right] \\ &= 2\,e^{\frac{\beta p_0}{2}}\int\frac{d^4k}{(2\pi)^2}\,f(k_0)\,f(p_0-k_0)\,\rho_{\phi\phi}(k_0,\mathbf{k})\,\rho_{\phi\phi}(p_0-k_0,\mathbf{p}-\mathbf{k})\,, \end{aligned} \tag{3.3}$$

with the Bose distribution

$$f(k_0) = \frac{1}{\exp(\beta k_0)-1}\,. \tag{3.4}$$

Combining this with Eqs. (3.2) and (3.1) we obtain

$$\eta_{\phi^2\phi^2}^{1-\text{loop}} = 2\beta \int \frac{d^4k}{(2\pi)^3}\, f(k_0)\,[1+f(k_0)]\,[\rho_{\phi\phi}(k_0,|\mathbf{k}|)]^2\,, \tag{3.5}$$

where we used Eq. (2.18) as well as the identity $f(-k_0) = -[1+f(k_0)]$. The factor β results from $\lim_{p_0\to 0}(e^{\beta p_0}-1)/p_0$. Up to a factor of 2π resulting from our different normalization (2.22) of the spectral density, this result is identical with the (much lengthier) calculation [5] from the cutting rules in ITF.

To further evaluate Eq. (3.5) we need the spectral density $\rho_{\phi\phi}(k_0,\mathbf{k})$ for the full single particle propagator. Since the calculation of $\eta_{\phi^2\phi^2}^{1-\text{loop}}$ requires taking the zero momentum limit of the loop diagram, both internal lines in Fig. 1 can become soft. For massless $\lambda\phi^4$ theory this means that, in order to avoid infrared divergences, we should use resummed effective propagators [3,7]. The so-called resummation of "hard thermal loops" [3] in this case generates a thermal mass for the scalar field which acts as an infrared cutoff. Using such a resummation scheme, we recently performed [8] a 2-loop calculation of $\rho_{\phi\phi}$. We found that for weak coupling among the scalar fields ($\lambda/24 \ll 1$) the spectral function is sharply peaked around the plasmon frequency

$$\omega_p(\mathbf{k}) = \sqrt{\mathbf{k}^2 + m_{\text{th}}^2 - \frac{3m_{\text{th}}^3}{\pi T}} \equiv \sqrt{\mathbf{k}^2 + m_{\text{p}}^2} \tag{3.6}$$

where

$$m_{\text{th}} = T\sqrt{\frac{\lambda}{24}} \tag{3.7}$$

is the "thermal mass" and m_{p} is the plasmon mass [7]. The spectral function $\rho_{\phi\phi}$ can then be expressed to good approximation in the form of a relativistic Breit-Wigner function,

$$\rho_{\phi\phi}(k_0,\mathbf{k}) \approx \frac{1}{\pi}\,\frac{2k_0\gamma(\mathbf{k})}{(k_0^2-\omega_p^2(\mathbf{k}))^2 + 4k_0^2\gamma^2(\mathbf{k})}\,, \tag{3.8}$$

where

$$\gamma(\mathbf{k}) = \frac{\text{Im}\,\Sigma(\omega_p(\mathbf{k}),\mathbf{k})}{2\omega_p(\mathbf{k})} \tag{3.9}$$

is the on-shell damping rate for the scalar plasmon. Its leading contribution comes from the 2-loop diagram in Fig. 2 and is given by [8,16]

$$\gamma(\mathbf{k}) = \frac{\lambda^2 T^2}{256\,\pi^3\,\omega_p(\mathbf{k})}\,\frac{1}{|\mathbf{k}|}\int_0^{|\mathbf{k}|} dq \Bigg[L_2(\xi) + L_2\left(\frac{\xi-\zeta}{\xi(1-\zeta)}\right) - L_2\left(\frac{\xi-\zeta}{1-\zeta}\right) - L_2\left(\frac{(\xi-\zeta)(1-\xi\zeta)}{\xi(1-\zeta)^2}\right)\Bigg]\,, \tag{3.10}$$

where

$$\xi = e^{-\beta\sqrt{\mathbf{k}^2+m_{\rm p}^2}}\,, \qquad \zeta = e^{-\beta\sqrt{\mathbf{q}^2+m_{\rm p}^2}}\,, \tag{3.11}$$

and $L_2(z)$ is the Spence function

$$L_2(z) \equiv -\int_0^z dt\,\frac{\ln(1-t)}{t}\,. \tag{3.12}$$

Substituting Eq. (3.8) into Eq. (3.5) and integrating over k_0 we obtain [1,5,17]

$$\eta_{\phi^2\phi^2}^{\rm 1-loop} \approx \frac{\beta}{2\pi}\int \frac{d^3k}{(2\pi)^3}\,\frac{f(\omega_p(\mathbf{k}))\,[1+f(\omega_p(\mathbf{k}))]}{\omega_p^2(\mathbf{k})\,\gamma(\mathbf{k})}\,. \tag{3.13}$$

IV. RESULTS AND DISCUSSION

We will now evaluate the momentum integral in (3.13). It can be studied analytically in the weak coupling limit $\lambda \ll 1$. Let us first consider an approximation which has been investigated before [2,5] where the momentum dependence of the plasmon width is neglected and $\gamma(\mathbf{k})$ is replaced by its zero-momentum limit

$$\gamma(0) = \frac{{\rm Im}\,\Sigma(m_{\rm p},0)}{2\,m_{\rm p}} = \frac{\lambda^2\,T^2}{256\,\pi^3\,m_{\rm p}}\,L_2(e^{-m_{\rm p}/T}) = \frac{\lambda^2 T^2}{1536\pi m_{\rm p}}\,\left[1+\mathcal{O}(\sqrt{\lambda}\ln\lambda)\right]\,. \tag{4.1}$$

Inserting this into Eq. (3.13) and integrating by parts leads to

$$\eta_{\phi^2\phi^2}^{\rm 1-loop}\Big|_{\gamma(\mathbf{k})=\gamma(0)} = \frac{384\,a^3}{\pi^2\,T\,\lambda^2}\int_0^\infty \frac{dx}{(x^2+a^2)^{3/2}}\,\frac{1}{e^{\sqrt{x^2+a^2}}-1}\,, \tag{4.2}$$

with $a = m_{\rm p}/T$. For small $a \ll 1$ the integral can be evaluated following the methods of Appendix C in Ref. [18], and we obtain [19]

$$\eta_{\phi^2\phi^2}^{\rm 1-loop}\Big|_{\gamma(\mathbf{k})=\gamma(0)} \approx \frac{96}{\pi T}\frac{1}{\lambda^2}\left(1-\sqrt{\frac{\lambda}{6\pi^2}}+\mathcal{O}(\lambda)\right)\,. \tag{4.3}$$

With the explicit momentum dependence [8] of the plasmon decay width from Eq. (3.10) this approximation can be avoided. Inserting Eq. (3.10) into Eq. (3.13) and integrating by parts, one finds

$$\eta_{\phi^2\phi^2}^{1-\mathrm{loop}} = \frac{64}{\lambda^2\, T} \int_0^\infty \frac{dx}{e^{\sqrt{x^2+a^2}} - 1} \, \frac{A(x;a) - xA'(x;a)}{A^2(x;a)} \tag{4.4}$$

where $x = k/T$, the prime denotes d/dx, and

$$\begin{aligned} A(x;a) &\equiv \frac{256\,\pi^3}{\lambda^2\, T^2}\, \omega_p(\mathbf{k})\, \gamma(\mathbf{k}) = \frac{128\,\pi^3}{\lambda^2\, T^2}\, \mathrm{Im}\, \Sigma(\omega_p(\mathbf{k}), \mathbf{k}) \\ &= \frac{1}{x} \int_0^x dz \, \left[L_2(\xi) + L_2\left(\frac{\xi-\zeta}{\xi(1-\zeta)}\right) - L_2\left(\frac{\xi-\zeta}{1-\zeta}\right) - L_2\left(\frac{(\xi-\zeta)(1-\xi\zeta)}{\xi(1-\zeta)^2}\right)\right] \end{aligned} \tag{4.5}$$

with (see Eq. (3.11))

$$\xi = e^{-\sqrt{x^2+a^2}}\,, \qquad \zeta = e^{-\sqrt{z^2+a^2}}\,, \quad \text{and} \quad a = \frac{m_{\mathrm{p}}}{T}\,. \tag{4.6}$$

The function $A(x;a)$ is shown in Fig. 3. For large momenta, $x \to \infty$, it approaches the constant value [16]

$$\begin{aligned} \lim_{x\to\infty} A(x;a) \;&=\; -\int_0^\infty dz\, \ln\left(1 - e^{-\sqrt{z^2+a^2}}\right) = \int_a^\infty \frac{\sqrt{\varepsilon^2 - a^2}\, d\varepsilon}{e^\varepsilon - 1} \\ &\longrightarrow \begin{cases} \pi^2/6 & \text{for } \; a \to 0\,; \\ aK_1(a) & \text{for } \; a \gg 1\,. \end{cases} \end{aligned} \tag{4.7}$$

At zero momentum it takes the value [16]

$$A(0;a) = L_2(e^{-a}) \tag{4.8}$$

which again approaches $\pi^2/6$ in the weak coupling limit $a = \sqrt{\lambda/24} \to 0$. Unfortunately, in the weak coupling limit the function $A(x;a)$ exhibits a very strong momentum dependence in the region $a < x < 1$; for $a = 0$ the limit $x \to 0$ is non-analytic. If we nonetheless neglect the momentum dependence of A, Eq. (4.4) becomes very simple:

$$\eta_{\phi^2\phi^2}^{1-\mathrm{loop}} \approx \frac{64}{\lambda^2\, T}\, \frac{6}{\pi^2} \int_0^\infty \frac{dx}{e^{\sqrt{x^2+a^2}} - 1}\,. \tag{4.9}$$

In the limit $a \to 0$ this integral diverges logarithmically in the infrared. The singular behaviour can be isolated by writing

$$\int_0^\infty \frac{dx}{e^{\sqrt{x^2+a^2}}-1} = \int_a^\infty \frac{\varepsilon}{\sqrt{\varepsilon^2-a^2}}\frac{d\varepsilon}{e^\varepsilon-1} = \int_a^\infty \frac{d\varepsilon}{e^\varepsilon-1} + \int_a^\infty \frac{\varepsilon-\sqrt{\varepsilon^2-a^2}}{\sqrt{\varepsilon^2-a^2}}\frac{d\varepsilon}{e^\varepsilon-1}$$
$$= -\ln(1-e^{-a}) + \int_a^\delta \frac{\varepsilon-\sqrt{\varepsilon^2-a^2}}{\sqrt{\varepsilon^2-a^2}}\frac{d\varepsilon}{\varepsilon} + \mathcal{O}\left(\frac{a^2}{\delta^2}\right)$$
$$= \ln\left(\frac{1}{a}\right) + \ln 2 + \mathcal{O}(a) + \mathcal{O}\left(\frac{a^2}{\delta^2}\right). \tag{4.10}$$

In the second line we cut off the second integral at the upper end at a point δ with $a \ll \delta \ll 1$. This allows to approximate the Bose distribution as $1/\varepsilon$. One easily verifies that the remaining integral from δ to ∞ is finite and of order a^2/δ^2 as indicated. We thus find with this approximation [19]

$$\eta_{\phi^2\phi^2}^{1-\text{loop}} \approx \frac{384}{\pi^2 T}\frac{1}{\lambda^2}\left(\ln\left(\frac{T}{m_\text{p}}\right) + \ln 2 + \mathcal{O}\left(\frac{m_\text{p}}{T}\right)\right)$$
$$= \frac{192}{\pi^2 T}\frac{1}{\lambda^2}\left(\ln\left(\frac{1}{\lambda}\right) + \ln(96) + \mathcal{O}\left(\sqrt{\lambda}\right)\right). \tag{4.11}$$

The additional logarithmic divergence in the weak coupling limit of (4.11) compared to (4.3) is generic; its coefficient and the next-to-leading constant term depend, however, on the momentum dependence of $A(x;a)$. Due to the non-analytic behaviour of $A(x;0)$ near $x=0$ we were not successful in extracting an analytical expression similar to (4.11) for the full integral (4.4). The numerical result shown by the dots in Figure 4 can, however, be excellently fit by

$$\eta_{\phi^2\phi^2}^{1-\text{loop}} \Big/ \eta_{\phi^2\phi^2}^{1-\text{loop}}\Big|_{\gamma(\mathbf{k})=\gamma(0)} = 0.3282\,\ln\left(\frac{T}{m_\text{p}}\right) + 1.41682 \approx \frac{1}{\pi}\,\ln\left(\frac{T}{m_\text{p}}\right) + \sqrt{2} \tag{4.12}$$

which suggests the analytical behaviour

$$\eta_{\phi^2\phi^2}^{1-\text{loop}} = \frac{96}{\pi^2 T}\frac{1}{\lambda^2}\left(\ln\left(\frac{T}{m_\text{p}}\right) + \pi\sqrt{2} + \mathcal{O}\left(\frac{m_\text{p}}{T}\right)\right)$$
$$= \frac{48}{\pi^2 T}\frac{1}{\lambda^2}\left(\ln\left(\frac{1}{\lambda}\right) + \ln(24) + 2\pi\sqrt{2} + \mathcal{O}\left(\sqrt{\lambda}\right)\right). \tag{4.13}$$

As intuitively expected, the viscosity decreases as the coupling strength increases: In relaxation time approximation all transport coefficients are proportional to the relaxation time, which again is inversely proportional to the scattering rate which grows with the coupling strength. On the other hand, the rate at which our $\eta_{\phi^2\phi^2}$ decreases with the

coupling strength λ is different from the behaviour of the physical shear viscosity η. As discussed in the Introduction, the latter involves four additional spatial derivatives acting on the scalar field. This translates [1] into an additional factor k^4 in the integrand of Eq. (3.13), which removes the infrared divergence of this integral in the limit $a \to 0$ and thereby also the leading logarithmic term in our final result (4.13). This observation provides a partial explanation for the qualitatively different behaviour of the viscosity as a function of $m_{\rm p}/T$ which was recently found by Jeon in a more complete study of $g\phi^3 + \lambda\phi^4$ theory [16]: his numerical results indicate an increase of $\lambda^2\eta$ with increasing λ.

Still, as first pointed out by Jeon in [5] and then quantitatively analyzed in [16], the fact that the shear viscosity η is proportional to $1/\lambda^2$ raises a serious problem: simple power counting arguments [5] show that then all planar ladder diagrams of the type shown in Fig. 5 can also contribute to the leading order result for the viscosity. The summation of this infinite series of ladder diagrams is nontrivial and has been recently performed by Jeon [16] using the imaginary time formalism. This work was a genuine *tour de force*, and the prospect of generalizing it to non-abelian gauge theories like QCD seems frightening. However, based on the results presented in this work, we believe that the methods developed here in the framework of TFD will help to redo the analysis in a more efficient way and allow for an easier generalization to QCD. Work in this direction is in progress.

ACKNOWLEDGMENTS

Two of authors (E.W. and X.Z.) are grateful to Liu Lianshou, Li Jiarong and R.D. Pisarski for helpful discussions. This work was supported in part by the Deutsche Forschungsgemeinschaft (DFG), the Bundesministerium für Bildung und Forschung (BMBF), the National Natural Science Foundation of China (NSFC) and the Gesellschaft für Schwerionenforschung (GSI).

REFERENCES

* On leave of absence from Institute of Particle Physics, Hua-Zhong Normal University, Wuhan, China.

[1] A. Hosoya, M.-A. Sakagami and M. Takao, Ann. Phys. (N.Y.) **154**, 229 (1984).

[2] S.V. Ilyin, A.D. Panferov, and Yu. Sinyukov, Phys. Lett. B**227**, 455 (1989); S.V. Ilyin, O.A. Mogilevsky, S. Smolyanski, and G.M. Zinovjev, Phys. Lett. B**296**, 385 (1992).

[3] R.D. Pisarski, Phys. Rev. Lett. **63**, 1129 (1989); E. Braaten and R.D. Pisarski, Nucl. Phys. B**337**, 569 (1990).

[4] D.N. Zubarev, *Nonequilibrium Statistical Thermodynamics*, (Plenum, New York, 1974).

[5] S. Jeon, Phys. Rev. D**47**, 4586 (1993).

[6] Y. Takahashi and H. Umezawa, Collec. Phen. **2**, 55 (1975); H. Umezawa, H. Matsumoto and M. Tachiki, *Thermo Field Dynamics and Condensed States* (North-Holland, Amsterdam, 1982).

[7] R.R. Parwani, Phys. Rev. D**45**, 4695 (1992).

[8] E. Wang and U. Heinz, *The plasmon in hot ϕ^4 theory*, Regensburg preprint TPR-95-3 (1995), submitted to Phys. Rev. D.

[9] R.L. Kobes and G.W. Semenoff, Nucl. Phys. B**260**, 714 (1985), and **272**, 329 (1986); R.L. Kobes, Phys. Rev. D**42**, 562 (1990), and **43**, 1269 (1991).

[10] M.A. van Eijck and Ch.G. van Weert, Phys. Lett. B**278**, 305 (1992).

[11] T.S. Evans, Nucl. Phys. B**374**, 340 (1992).

[12] H. Lehmann, Nuovo Cimento **11**, 342 (1954).

[13] H.A. Weldon, Phys. Rev. D**28**, 2007 (1983).

[14] H. Matsumoto, I. Ojima and H. Umezawa, Ann. Phys. (N.Y.) **152**, 348 (1984).

[15] Y. Fujimoto, M. Morikawa and M. Sasaki, Phys. Rev. D**33**, 590 (1986).

[16] S. Jeon, *Hydrodynamic transport coefficients in relativistic scalar field theory*, University of Washington preprint UW/PT 94-09, unpublished.

[17] Yu.S. Gangnus, A.V. Prozorkevich, and S.A. Smolyanskii, Theor. Math. Phys. **35**, 321 (1978).

[18] L. Dolan and R. Jackiw, Phys. Rev. D**9**, 3320 (1974).

[19] Our result should be compared with Eq. (5.12) in Ref. [5]. If in that expression the mass is replaced by the thermal mass $m_{\rm th}$ or $m_{\rm p}$, it exhibits a logarithmic dependence $\sim \lambda^{-2}\ln(a\lambda)$ on the coupling constant. In [5] it is stated that this result (with $a = 2$) is obtained if the momentum dependence of the plasmon *width* is neglected; this disagrees with our result (4.3) in that limit. Jeon's result (5.12) with $a = 2$ is, however, recovered if the momentum dependence of the imaginary part of the plasmon's *self energy* is neglected, see our Eq. (4.11).

FIGURES

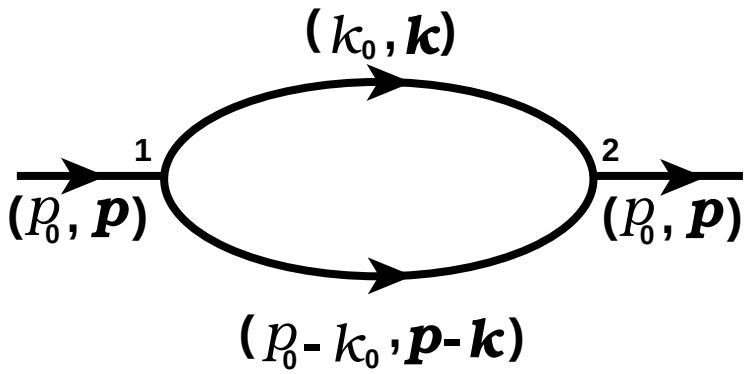

FIG. 1. One-loop skeleton diagram for $\Delta^{12}_{\phi^2\phi^2}(p_0, \mathbf{p})$. The heavy lines denote full single particle propagators.

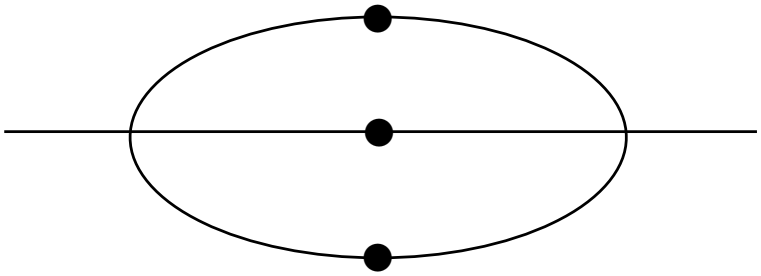

FIG. 2. The leading contribution to the imaginary part of self energy $\mathrm{Im}\,\Sigma$. The dotted lines denote resummed effective propagators.

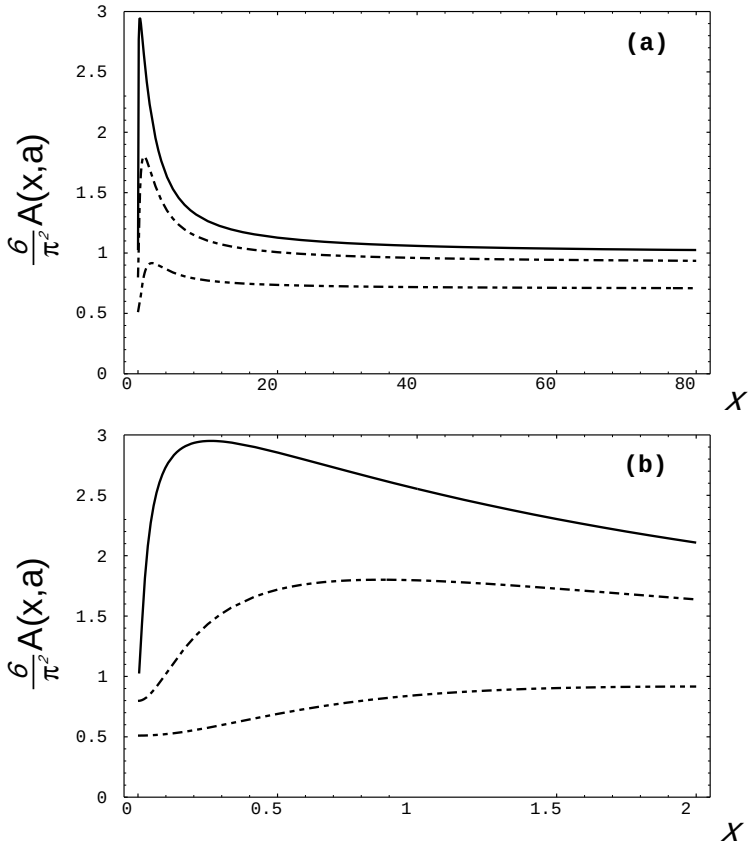

FIG. 3. (a) The function $(6/\pi^2)A(x;a)$ vs. x for $a = 0.01$, 0.1, and 0.4 (from top to bottom). (b) Close-up of (a) for small x.

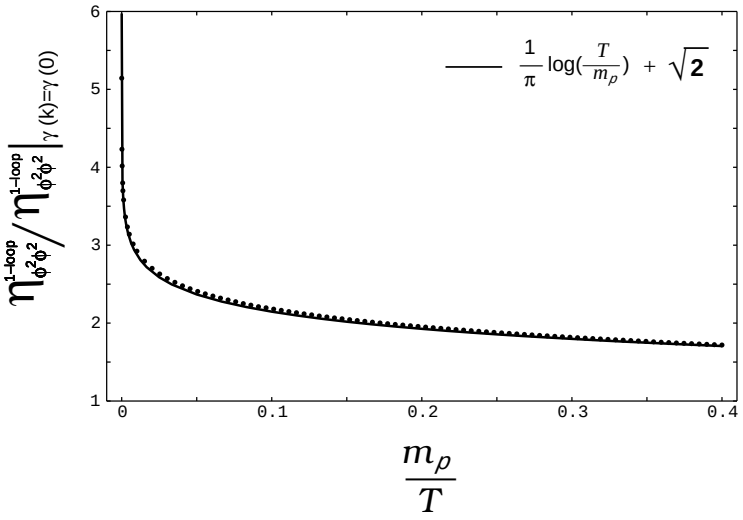

FIG. 4. The dots represent numerical results for the ratio between $\eta^{1-\text{loop}}_{\phi^2\phi^2}$ and $\eta^{1-\text{loop}}_{\phi^2\phi^2}\Big|_{\gamma(\mathbf{k})=\gamma(0)}$ as a function of m_p/T. The solid line indicates a fit of the form $(1/\pi)\ln(T/m_\text{p}) + \sqrt{2}$.

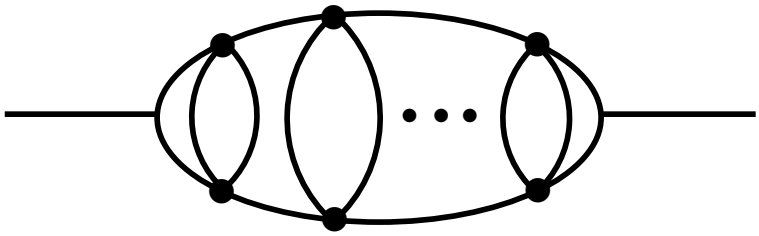

FIG. 5. The multi-loop planar-ladder skeleton diagram in $\lambda\phi^4$ theory.